# FRACTIONAL DUAL-PHASE-LAG HEAT CONDUCTION WITH PERIODIC HEATING AND PHOTO-THERMAL RESPONSE

by

## Aloisi SOMER[a], Andressa NOVATSKI[a], Marcelo K. LENZI[b], Luciano R. da SILVA[c,d], and Ervin K. LENZI[a,d*]

[a] Departamento de Fisica, Universidade Estadual de Ponta Grossa, Ponta Grossa, Brazil
[b] Departamento de Engenharia Quimica, Universidade Federal do Parana, Curitiba, Brazil
[c] Departamento de Fisica, Universidade Federal do Rio Grande do Norte, Natal, Brazil
[d] National Institute of Science and Technology for Complex Systems,
Centro Brasileiro de Pesquisas Fisicas, Rio de Janeiro, Brazil

*We apply an extension of dual-phase-lag in thermal systems to predict the photoacoustic signal for transmission configuration and characteristics of the open photoacoustic cell technique. For this, we consider a particular case from Jeffrey's equation as an extension of the generalized Cattaneo equations. In this context, we obtain the temperature distribution under the effects of fractional differential operators, allowing the calculation of the Photoacoustic signal for the transmission set-up. The results show a rich class of behaviors related to the anomalous diffusion connected to these fractional operators.*

Key words: *fractional dynamics, generalized Cattaneo equation, anomalous diffusion*

## Introduction

Diffusion is an intriguing natural phenomenon observed in different contexts, ranging from biology to physics [1, 2]. One of the characteristics of this process is the linear time dependence of the mean square displacement, *i.e.*, $\langle (z - \langle z \rangle)^2 \rangle$ by $t$, which is connected to the Markovian aspects of this stochastic process. However, many different contexts have exhibited another behavior for the mean square displacement, *e.g.*, $\langle (z - \langle z \rangle)^2 \rangle$ by $t^\alpha$, (where $\alpha$ less, equal, and greater than one corresponds to sub-, normal-, and super-diffusive) or $\langle (z - \langle z \rangle)^2 \rangle \sim \ln^\alpha t$ (related to an ultraslow diffusion [3]), by evidencing the presence of non-Markovian processes [4, 5]. Anomalous processes in heat transfer [6, 7] have been analyzed by using extensions of the Fourier law [8, 9] to overcome problems related to low temperature conditions, non-homogenous materials, high intensity flux sources, spatial micro-scales [7, 10], and among others. One of the approaches used to analyze anomalous heat transfer employs fractional calculus. This approach has brought insights and becomes a new efficient mathematical tool to analyze different properties of systems and connect them with the experimental results. Compte and Metzler [11] proposed some forms of generalizing the Cattaneo equation (GCE) using fractional operators in time. Each one was supported by continuous-time random walks, non-local transport theory, and delayed flux-force relation [9, 11]. In particular, the photo-thermal phenomena area has been interested in the application of hyperbolic [12, 13], double relaxation [14], and fractional

Somer, A., *et al.*: Fractional Dual-Phase-Lag Heat Conduction with Periodic ...
THERMAL SCIENCE: Year 2023, Vol. 27, No. 3B, pp. 2537-2547

2538

[15, 16] models to approximate the predictions of the photoacoustic (PA) signal to the experimental results. The analyzed photo-thermal responses allow for obtaining the thermal characteristics, especially the solid materials investigated using the PA signal [17, 18]. The PA signal responds to excitation by periodically modulated radiation as a pressure fluctuation in the gas close to the sample [19, 20]. The open photoacoustic cell (OPC) is a photo-thermal technique that analyses the PA signal as a function of the frequency of thermal excitation by using a transmission configuration where the excitation and detection are on opposite sides of the sample [21, 22]. A dual-phase-lag (DPL) for the hyperbolic diffusion equation was developed from complex heat capacity in the energy conservation law with experimental correspondence to the photoacoustic response in the OPC technique [23].

Here, we apply an extension of DPL in thermal systems by considering the fractional differential operators to predict the PA signal for transmission configuration and characteristics of the OPC technique. We use a particular case originating from Jeffrey's equation, an extension of the GCE-I model with a fractional DPL [24]. It is worth mentioning that extensions of the DPL have successfully been applied to heat conduction with insights to explain anomalous thermal behaviors [24-26]. We also obtain the 1-D temperature variation for the photo-thermal phenomena from fractional thermal diffusion by considering a planar light excitation. The results show a large class of behaviors and the strengthening of the effects of superdiffusion or subdiffusion [24], which can elucidate experimental results not contemplated by GCE's generalizations [27].

## The fractional dual-phase-lag diffusion equation

The heat flux $\mathbf{q}(\mathbf{r}, t)$ at a given position in space at a given time is related to the temperature gradient $\nabla T(\mathbf{r}, t)$ according to the Fourier Law:

$$\mathbf{q}(\mathbf{r}, t) = -k\nabla T(\mathbf{r}, t) \tag{1}$$

where $k$ is the thermal conductivity. A generalization of eq. (1) was proposed by Cattaneo [8] by considering a phase-lag in heat flux by the addition of a relaxation time $\tau_q$:

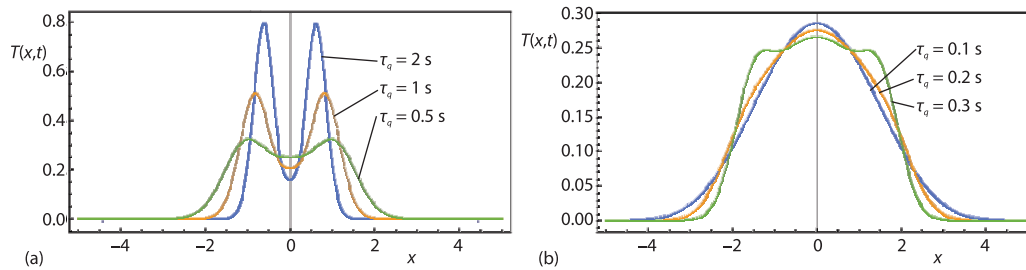$$\mathbf{q}(\mathbf{r}, t + \tau_q) = -k\nabla T(\mathbf{r}, t) \tag{2}$$

which approximated in first order yields $(1 + \tau_q \partial t)\mathbf{q}(\mathbf{r}, t) = -k \nabla T(\mathbf{r}, t)$, where $\partial t$ is the first order time partial derivative. The DPL model of heat conduction was suggested by Tzou [28], by considering a second relation time $\tau_T$ in the temperature gradient, which implies:

$$\mathbf{q}(\mathbf{r}, t + \tau_q) = -k\nabla T(\mathbf{r}, t + \tau_T) \tag{3}$$

The first order approximation for eq. (3) results:

$$\left(1 + \tau_q \partial_t\right)\mathbf{q}(\mathbf{r}, t) = -k(1 + \tau_T \partial_t)\nabla T(\mathbf{r}, t) \tag{4}$$

with additional terms connected with the relaxation times $\tau_q$ and $\tau_T$. Equation (4) recovers the Fourier law in the limit $\tau_q \rightarrow 0$ and $\tau_T \rightarrow 0$. Figure 1 illustrates the behavior of the solution for the 1-D case, obtained from eq. (4) combined with the continuity equation in the absence of external forces and source (or sink) terms. It shows that each relaxation time influences the spreading of the system, and a different behavior is obtained for $\tau_T \neq 0$ and $\tau_q \neq 0$, in contrast to the particular cases $\tau_T = 0$ and $\tau_q = 0$. Figure 1 illustrates the different behaviors which can be obtained depending on the choices performed to $\tau_T$ or $\tau_q$. It is worth mentioning that the DPL model has been applied in several situations, such as bioheat transfer of cardiac ablation [29], the temperature in living tissue [30], and thermal damage to skin tissue subjected to moving heat source [31], see also [32] for additional discussions.

Somer, A., *et al.*: Fractional Dual-Phase-Lag Heat Conduction with Periodic ...
THERMAL SCIENCE: Year 2023, Vol. 27, No. 3B, pp. 2537-2547

2539

**Figure 1. Behavior of eq. (4) combined with the continuity equation for $T(x, t)$ different values of $\tau_T$ and $\tau_q$; we consider, for simplicity, $k = 1$; (a) $\tau_T = 0.1$ seconds and (b) $\tau_T = 0.05$ seconds**

Equation (4) has also been extended by considering the fractional differential operator [24], which has been proven to be a useful mathematical tool for describing the kinetics of many strange physical phenomena [33-35]. The extension considered here, fractional dual-phase-lag (FDPL), is based on the Jeffreys-type equation [24]:

$$\left(1 + \tau_q^\alpha \partial_t^\alpha\right)\mathbf{q}(\mathbf{r},t) = -k_\gamma \partial_t^{1-\gamma}\left(1 + \tau_T^\beta \partial_T^\beta\right)\nabla T(\mathbf{r},t) \tag{5}$$

where $0 < \alpha, \beta, \gamma < 1$, and $k_\gamma = k\tau_q^{1-\gamma}$, and $\partial_t^\alpha$ is the Caputo fractional derivative or integral:

$$_{t_0}\partial_t^\gamma f(x,t) = \begin{cases} \dfrac{1}{\Gamma(1-\gamma)}\displaystyle\int_{t_0}^t \dfrac{\mathrm{d}t'}{(t-t')^\gamma}\dfrac{\partial}{\partial t}f(x,t'), & \text{for } 0 < \gamma < 1 \\[12pt] \dfrac{1}{\Gamma(-\gamma)}\displaystyle\int_{t_0}^t \mathrm{d}t'\dfrac{f(x,t')}{(t-t')^{1+\gamma}}, & \text{for } \gamma < 0 \end{cases} \tag{6}$$

respectively. The DPL represented by eq. (4) is recovered when $\alpha = \beta = \gamma = 1$. A special case of Jeffreys-type equation analyzed in [25] is the GCE-I Compte-Metzler equation obtained for $\alpha = \gamma$, as an extension FDPL-GCE-I:

$$\left(1 + \tau_q^\alpha \partial_t^\alpha\right)\mathbf{q}(\mathbf{r},t) = -k_\alpha \partial_t^{1-\alpha}\left(1 + \tau_T^\beta \partial_t^\beta\right)\nabla T(\mathbf{r},t) \tag{7}$$

Also, the validity interval is generalized, following Jeffrey's equations, with $0 \le \alpha, \beta \le 1$. If $\beta = 1$ and $\tau_T = 0$ in the eq. (7), the original GCE I with one-phase-lag is recovered:

$$\left(1 + \tau_q^\alpha \partial_t^\alpha\right)\mathbf{q}(\mathbf{r},t) = -k_\alpha \partial_t^{1-\alpha}\nabla T(\mathbf{r},t) \tag{8}$$

The thermal diffusion equation is obtained by combining the Fourier Law, eq. (1) with the Energy Conservation Law:

$$\rho c_p \partial_t T(\mathbf{r},t) + \nabla \mathbf{q}(\mathbf{r},t) = F(\mathbf{r},t) \tag{9}$$

where $F(r, t)$, $\rho$, and $c_p$ are the heat source, density, and specific heat, respectively. The classical thermal diffusion (CTD):

$$D\nabla^2 T(\mathbf{r},t) - \partial_t T(\mathbf{r},t) = -\left(\frac{D}{k}\right)F(\mathbf{r},t) \tag{10}$$

where the standard thermal diffusivity is defined as $D = k/\rho c_p$. For the general case, from Jeffreys-type equation, eq. (5), the thermal diffusion equation:

$$D_\gamma \partial_t^{1-\gamma}\left(1 + \tau_T^\beta \partial_t^\beta\right)\nabla^2 T(\mathbf{r},t) - \left(1 + \tau_q^\alpha \partial_t^\alpha\right)\partial_t T(\mathbf{r},t) = -\left(\frac{D_\gamma}{k_\gamma}\right)\left(1 + \tau_q^\alpha \partial_t^\alpha\right)F(\mathbf{r},t) \tag{11}$$

with the fractional thermal diffusivity defined as $D = k_\gamma/\rho c_p$. For the FDPL-GCE-I, by combining eq. (7) with eq. (9) the generalized thermal diffusion equation is obtained:

$$D_\alpha \left(1 + \tau_T^\beta \partial_t^\beta\right)\nabla^2 T(\mathbf{r},t) - \partial_t^{\alpha-1}\left(1 + \tau_q^\alpha \partial_t^\alpha\right)\partial_t T(\mathbf{r},t) = -\left(\frac{D_\alpha}{k_\alpha}\right)\partial_t^{\alpha-1}\left(1 + \tau_q^\alpha \partial_t^\alpha\right)F(\mathbf{r},t) \tag{12}$$

The anomalous thermal conductivity, $k_\alpha$, has dimensions [kgms$^{-2-\alpha}$K$^{-1}$] and the anomalous thermal diffusivity, $D_\alpha$, has dimension [m$^2$s$^{-\alpha}$]. In this manner, eq. (12) extends the previous ones to a general situation and has a large class of behaviors, which can be connected to anomalous diffusion.

**The photoacoustic problem**

A pressure variation is recorded in the PA procedures due to heat transfer from the sample to the neighboring gas, known as the PA signal. For transmission set-up configuration the pressure variation is [15, 19, 20]:

$$\delta P = \frac{\Gamma P_0}{T_0 l_g \sigma_g} T_s\left(\frac{l_s}{2}\right) \tag{13}$$

where $\Gamma$ is the air specific heat ratio, $P_0$ – the atmospheric pressure, $T_0$ – the ambient temperature, $l_g$ – the thickness of the gas chamber, and $l_s$ – the sample thickness, $T_s(l_s/2)$ – the sample temperature variation at interface sample-air closed to the cell, and $\sigma_j$ – the complex medium thermal diffusion length, with $j = g, b$ for the surrounding air and $j = s$ for the sample, given by: $\sigma_j = (i\omega/D_j)^{1/2}$.

By considering that the absorption of radiation by air is negligible, so the heat source is present only in the sample, with $F_b = F_g = 0$, and: $F_s(z, t) = \eta_s I_0 \lambda_s e^{-\lambda_s z} e^{i\omega t}$, with $\omega = 2\pi f$, in which $f$ – the frequency of light modulation, $\lambda_s$ – the optical absorption coefficient, $I_0$ – the light intensity, and $\eta_s$ – the quantum coefficient of the electromagnetic energy to heat conversion of the sample, that we consider $\eta_s = 1$.

The PA signal is monitored at the same frequency as the heat source. Thus, the temperature variation in the three media must have the same shape as the source, and the temporal solution is well defined and written as $T(z, t) = \theta(z)e^{i\omega t}$. Due to the experimental characteristics, we consider the stationary case with the initial condition $t_0 = -\infty$, where $\partial_t^\gamma e^{i\omega t} = (i\omega)^\gamma e^{i\omega t}$ [34]. Also, the PA problem can be approximated for the 1-D case because the light heating is uniformly distributed with a spot larger than the sample radius [20]. The temperature variation profile of the sample $T_s(z, t)$ is obtained by solving the 1-D set diffusion equations [15]:

$$\frac{d^2}{dz^2}\theta_j(z) - \frac{m_j}{D_{\alpha_j}}(i\omega)\theta_j(z) = -\frac{m_j}{k_{\alpha_j}}F_j(z) \tag{14}$$

with $j = b, s, g$ for backing air, sample, and air closed in PA cell, respectively, and $m_j$ – the obtained from FDPL-GCE-I (12) temporal fractional derivatives applied to periodical temperature solution $e^{i\omega t}$, resulting:

$$m_j = \frac{(i\omega)^{\alpha_j - 1}\left(1 + \tau_{qj}^{\alpha_j}(i\omega)^{\alpha_j}\right)}{1 + \tau_{Tj}^{\beta_j}(i\omega)^{\beta_j}} \tag{15}$$

The boundary conditions are the zero temperature variation in system borders at $z = \pm\infty$, continuity of temperature, and also heat flux at the interfaces backing air-sample ($z = -l_s/2$), and sample-air inner the PA cell ($z = l_s/2$):

$$\theta_b(-\infty) = 0, \ \theta_g(\infty) = 0, \ \theta_b\left(z = \frac{-l_s}{2}\right) = \theta_s\left(z = \frac{-l_s}{2}\right), \ \theta_s\left(z = \frac{-l_s}{2}\right) = \theta_g\left(z = \frac{-l_s}{2}\right) \tag{16}$$

and

$$k_{\alpha g} \frac{\mathrm{d}}{\mathrm{d}z}\theta_b(z)\Big|_{z=-\frac{l_s}{2}} = k_{\alpha s} \frac{\mathrm{d}}{\mathrm{d}z}\theta_s(z)\Big|_{z=-\frac{l_s}{2}}, \ k_{\alpha s} \frac{\mathrm{d}}{\mathrm{d}z}\theta_s(z)\Big|_{z=\frac{l_s}{2}} = k_{\alpha g} \frac{\mathrm{d}}{\mathrm{d}z}\theta_g(z)\Big|_{z=\frac{l_s}{2}} \tag{17}$$

By solving the previous equations and assuming that:
– the thermal effusivity, $e = (k\rho c)^{1/2}$, of the sample is much greater than the one air [19];
– the fractional-order derivatives for air are $\alpha = \beta = 1$; and
– the two relaxation times of air are small, $\tau_q \rightarrow 0$ and $\tau_T \rightarrow 0$; the temperature in the sample is founded:

$$T_s(z,t) = \frac{I_0 \cosh\left[\sigma_{m_s}\left(z - \frac{l_s}{2}\right)\right]H_s(z,\beta)e^{i\omega t}}{k_{m_s} \sinh\left(\sigma_{m_s} l_s\right)} \tag{18}$$

where

$$k_{m_s} = \frac{k_s}{m_s}, \ \sigma_{m_s} = m_s^{1/2}\sigma_s, \ \text{and} \ H_s(z,\beta) = \Lambda_1(z,\beta) - \Lambda_2(z,\beta)$$

is the optical absorbing contribution, which tends to unit for opaque approach

$$\lim_{\beta \rightarrow \infty} H_s(z,\beta) = 1$$

The functions $\Lambda_1$ and $\Lambda_2$ are defined:

$$\Lambda_1(z,\beta) = \frac{1 - e^{-\beta l_s}\cosh\left[\sigma_{m_s}\left(\frac{l_s}{2} + z\right)\right]\operatorname{sech}\left[\sigma_{m_s}\left(z - \frac{l_s}{2}\right)\right]}{1 - \frac{\sigma_{m_s}^2}{\beta^2}} \tag{19}$$

$$\Lambda_2(z,\beta) = \frac{\sigma_{m_s} e^{-\beta\left(\frac{l_s}{2}+z\right)}\sinh\left(l_s\sigma_{m_s}\right)\operatorname{sech}\left[\sigma_{m_s}\left(z - \frac{l_s}{2}\right)\right]}{\beta\left(1 - \frac{\sigma_{m_s}^2}{\beta^2}\right)} \tag{20}$$

The pressure variation $\delta(P_{TD})$ due to heat diffusion for a transparent sample is given:

$$\delta P_{TD} = \frac{C_1 m_s e^{i\left(\omega t - \frac{\pi}{4}\right)}}{\sqrt{f}\sigma_{m_s}\sinh\left(l_s\sigma_{m_s}\right)}\frac{1}{1 - \frac{\sigma_{m_s}^2}{\beta^2}}\left[1 - e^{-\beta l_s}\cosh\left(l_s\sigma_{m_s}\right) - \frac{\sigma_{m_s}}{\beta}e^{-\beta l_s}\sinh\left(l_s\sigma_{m_s}\right)\right] \tag{21}$$

where

$$C_1 = \frac{\Gamma I_0 P_0 \sqrt{D_g}}{\sqrt{2\pi}l_g T_0 k_s}$$

Somer, A., *et al.*: Fractional Dual-Phase-Lag Heat Conduction with Periodic ...
THERMAL SCIENCE: Year 2023, Vol. 27, No. 3B, pp. 2537-2547

2542

is the amplitude of thermal diffusion contribution and your unit in the S.I. is $[C_1] = \mathrm{Pam^{-1}s^{-1/2}}$. For opaque samples ($\beta \to \infty$), and classical approach with $\tau_q \to 0$, $\tau_T \to 0$, $\alpha = 1$ and $\beta = 1$, the PA signal (pressure variation's non-temporal component) returns to equation founded by Rousset e coworkers [36], in rear incidence configuration, characteristic of OPC technique [20]:

$$\delta P_{TD} = \frac{C_1 e^{-i\frac{\pi}{4}}}{\sqrt{f}\,\sigma_s \sinh(\sigma_s l_s)}$$

## Results

The phase velocity $v_{ph}$ of the generated thermal wave is inversely proportional to the real component of the thermal conductivity, given by [11, 16, 37]:

$$v_{ph} = \frac{\omega}{\mathrm{Re}[k_{m_s}]} = \left(\frac{\omega}{k_s}\right)\mathrm{Re}[m_s]$$

As a result, the $v_{ph}$ is proportional to the $m_s$ factor's real component. The subdiffusive and superdiffusive behaviors can be determined by comparing the fractional models for $v_{ph}$ with the classical models. It is superdiffusive if the $v_{ph}$ is greater than the classical value and superdiffusive if it is less.
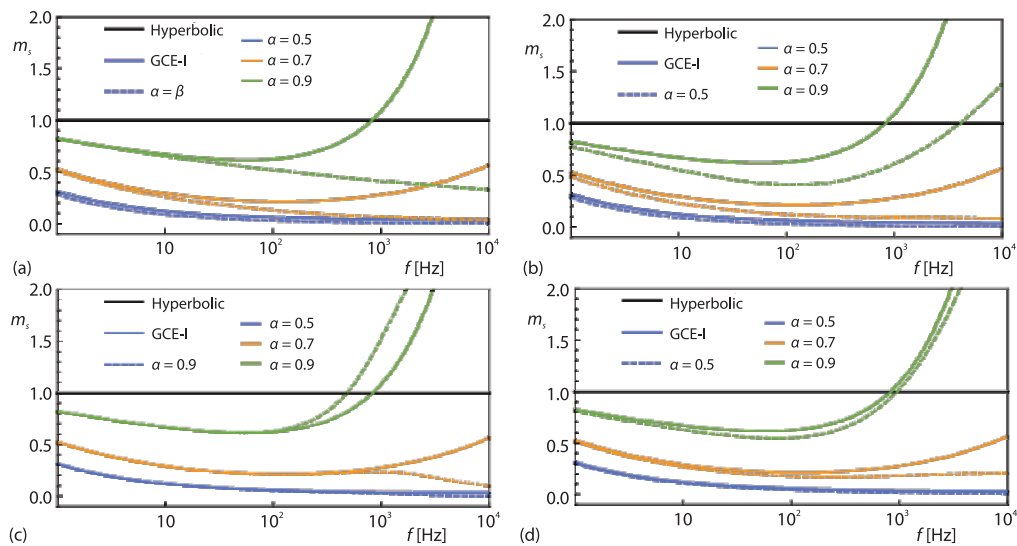


**Figure 2. Real component of the $m_s$ factor as a function of modulation frequency, $f$, and fractional derivative order $\alpha$ with; (a) $\tau_q = \tau_T = 10^{-3}$ seconds, and $\alpha = \beta$, (b) $\tau_q = \tau_T = 10^{-3}$ seconds, and $\beta = 0.5$, (c) $\tau_q = 10^{-3}$ seconds, $\tau_T = 10^{-4}$ seconds, and $\beta = 0.9$, and (d) $\tau_q = 10^{-3}$ seconds, $\tau_T = 10^{-4}$ seconds, and $\beta = 0.5$; the solid lines represent the GCE-I result, the dashed lines are the Fractional DPL model, and the solid black line is the hyperbolic case**

Figure 2 presents the real value of the $\mathrm{Re}[m_s]$ factor as a function of modulation frequency and fractional derivative order $\alpha$ for $0 < \alpha < 1$ for FDPL-GCE-I. The models converge to the hyperbolic when $\alpha = \beta = 1$, represented by the solid black line. The GCE-I model results are represented by solid lines and merged FDPL-GCE-I results by dashed lines. These results are suitable for photo-thermal processes, provided that the frequency modulation varies in most cases. Using these data, we can investigate the interval of sub and superdiffusive regimes for each operator. Figure 2 reveals that the factor $m_s$ for both operators in most frequency values present

Somer, A., *et al*.: Fractional Dual-Phase-Lag Heat Conduction with Periodic ...
THERMAL SCIENCE: Year 2023, Vol. 27, No. 3B, pp. 2537-2547

2543

results less than $m_s < 1$, implying that the phase velocity, $v_{ph}$, is lower than the thermal wave generated by the hyperbolic solution, which is indicative of the subdiffusive regime. However, there is a frequency cutoff, $f_c$, according to previous work [16], for which the operators change the behavior from subdiffusive to superdiffusive. The $f_c$ value increases with both $\tau$ and $\alpha$ increasing, and now in influenced by $\tau_T$ and $\beta$. All results show that the second phase-lag added in temperature gradient $\tau_T$ significantly influences phase velocity, mainly for higher frequencies. The influence is less for lower $\alpha$ values when the FDPL-GCE-I have similar values to GCE-I. Figures 2(a) and 2(b) reveal that high values of second relaxation time $\tau_T$ tend to keep the subdiffusion in all frequency ranges. At the same time, figs. 2(c) and 2(d) demonstrate that short second relaxation time $\tau_T$ increases the superdiffusion. The FDPL-GCE-I exhibits superdiffusive behavior for high alpha values when not in the long-time domain ($t > \tau_q$), *i.e.*, for high frequency.

The influence of the DPL in GCE-I is shown in fig. 3, with the absolute value of the temperature profile normalized by ($k_s T_s(z)/I_0$). The results are obtained for an opaque sample of thickness $l_s = 400$ µm and thermal diffusivity $\alpha_s = 40 \cdot 10^{-6}$, in the function of position $z$ and fractional order derivative, $\alpha$, heated by a uniform light source at $z = -l_s/2$ with frequency $f = 10^3$ Hz. These numbers were chosen to show how the factor $m_s$, and hence the fractional factor $\alpha$, affect temperature distribution. All simulations were performed until the establishment of attenuation for the subdiffusive behavior that occurs around the $0.5 < \alpha < 1$ interval.
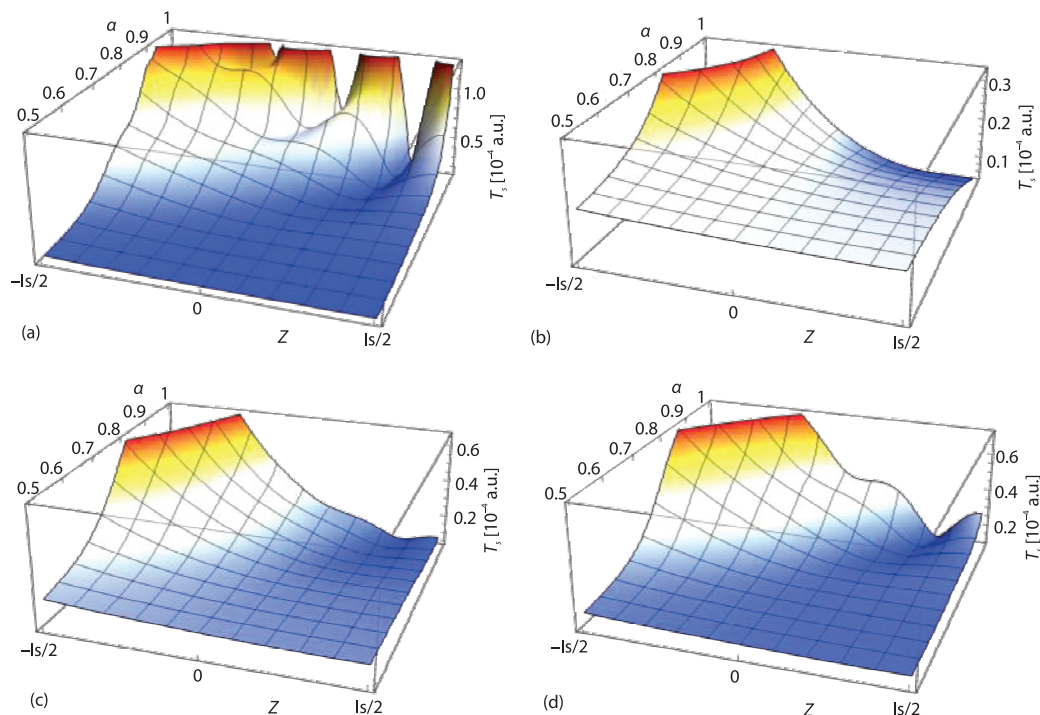


**Figure 3. Normalized ($k_s T_s(z)/I_0$) absolute value of the temperature distribution of an opaque sample heated by a light source at $z = -l_s/2$ as a function of ($\gamma$) with $l_s = 400$ µm, $f = 1000$ Hz and $D_s = 40 \cdot 10^{-6}$ m²/s; the temperature profile for (a) GCE-I with $\tau_q = 10^{-3}$ seconds, and FDPL-GCE-I for (b) special case with $\alpha = \beta$ and $\tau_q = \tau_T = 10^{-3}$ seconds, (c) $\beta = 0.9$, $\tau_q = 10^{-3}$ seconds, and $\tau_T = 10^{-4}$ seconds, and (d) $\beta = 0.5$, $\tau_q = 10^{-3}$ seconds, and $\tau_T = 10^{-4}$ seconds**

Figure 3(a) is the temperature in the sample, $T(z)$, calculated by using one-phase-lag GCE-I, *i.e.*, ($\tau_T \rightarrow 0$ and $\beta = 1$). It is observed around $\alpha = 1$ a resonant frequency, characteristic of hyperbolic result [18]. The frequency value of $f = 10^3$ Hz was set to see the superdiffusive contribution from fig. 2(a). When superdiffusive behavior is present, the resonant frequency becomes more prominent [38]. Figure 3(b) shows the result for the special case of FDPL-GCCE-I with $\alpha = \beta$ and for similar relaxation times, *i.e.*, $\tau_q - \tau_T = 10^{-3}$ seconds, as in fig. 2(a). As a result of this approach, the strongest subdiffusive outcome of all the evaluated data is obtained. No resonant frequency is observed even for $\alpha \rightarrow 1$. With the addition of the second derivative order $\beta$, the subdiffusive becomes less effective, and the resonant frequency is observed for $\alpha \rightarrow 1$, as can be seen in figs. 3(c) and 3(d). These results used short relaxation time for the temperature gradient, with $\tau_q = 10^{-3}$ seconds and $\tau_T = 10^{-4}$ seconds. Also, these results show that the decreases in $\beta$ value become more evident in the superdiffusion around $\alpha = 1$.
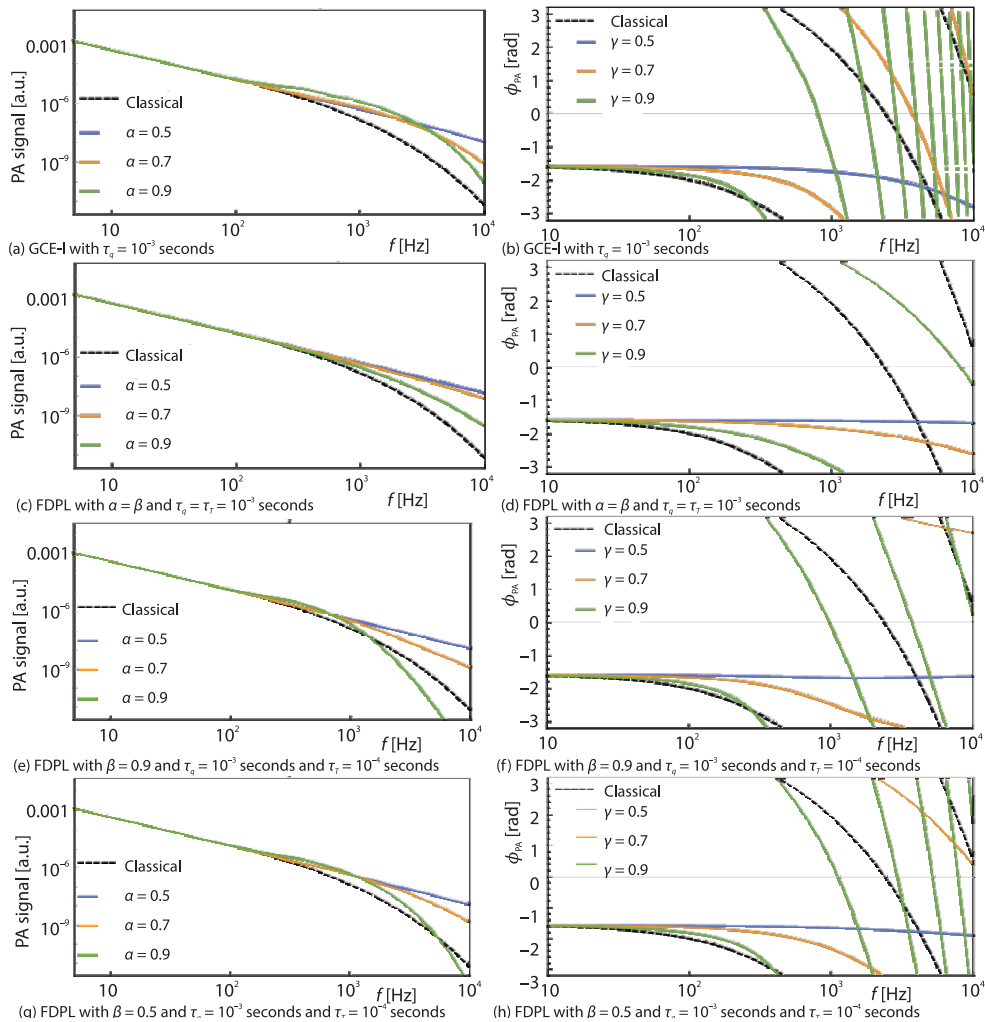


**Figure 4. The PA signal amplitude $|\delta P|$ in (a), (c), (e), and (g) and phase delay $\phi$ in (b), (d), (f) and (h) for FDPL-GCE-I as the function of f and $\alpha$ with $l_s = 400$ μm, $40 \cdot 10^{-6}$ m²/s and $\tau_q = 10^{-3}$ seconds**

Figure 4 presents the influence of the FDPL-GCE-I on the PA signal amplitude $|\delta P|$ figs. 4(a), 4(c), 4(e), and 4(g) and phase delay $\phi$ figs. 4(b), 4(d), 4(f), and 4(h). In all the results, it was used the opaque approach with constant thermal diffusivity and thickness at $40 \cdot 10^{-6}$ m²/s and $l_s = 400$ µm and $\tau_q = 10^{-3}$ seconds, to verify the influence of relaxation time $\tau_T$, and fractional orders $\alpha$ and $\beta$ under PA signal. The amplitude constant of the PA signal was used as $C_1 = 10^1$.

The amplitude of the PA signal for the GCE-I and the phase delay are shown in fig. 4(a). In fig.4 (b), we perform a comparison of the FDPL-GCE-I. When the PA signal amplitude is analyzed, the classical results show a characteristic frequency $f_c$ at which a behavioral change occurs. Linear behavior is achieved when $f < f_c$ is obtained, and an exponential decay is obtained for $f > f_c$. The characteristic frequency is obtained from $f_c = D_s/(\pi l_s^2)$, which for or case is $f_c = 80$ Hz. Also, the PA signal phase delay $\phi$ presents a significant variation, and a phase inversion is observed from $\pi$ to $-\pi$ [19, 20]. The one-phase-lag added to the heat flux that constructs the hyperbolic heat diffusion produces periodic oscillations in the PA signal amplitude after a resonant frequency, which depends on relaxation time $\tau_q$ and decreases the phase inversion frequency [18, 39, 40]. When the subdiffusion is present in all the frequency ranges (in presented results for $\alpha \le 0.7$), the $f_c$ value shift to high values, and linear behavior is observed for higher frequencies than the classical result. The superdiffusion act decreases the resonant frequency, and the oscillations in the PA signal are observed for frequencies lower than in hyperbolic results. This effect also increases the oscillation of phase inversion [15, 16].

In the special case analyzed in this work in which the derived GCE-I with the addition of the second phase-lag on temperature gradient and a second fractional-order derivative from Jeffrey's equation, the results reveal that the FDPL has a strong influence on the PA signal. The special case for $\alpha = \beta$, shown in figs. 4(c) and (d), is the most subdiffusive result. Thus, the resonant frequency and oscillations in PA signal amplitude are not observed. Also, the linear behavior and $f_c$ increases for lower $\alpha$. The phase inversion also is shifted to high frequencies.

For short gradient temperature relaxation time, $\tau_T = 10^{-4}$ seconds, figs. 4(e)-4(h) shows that the second phase-lag order derivative $\beta$ variation has a small influence on PA signal for lower frequencies. However, for higher frequency values, the influence of exponential decay is significant, revealing the main region of influence of the FDPL-GCE-I. This influence is more evident in phase delay $\phi$ than amplitude $|\delta P|$, once the linear behavior in the $\phi$ ($f > 10^2$ Hz) occurs for lower than $|\delta P|$ ($f > 10^3$ Hz).

The PA signal fluctuation is abrupt for the superdiffusive behavior. For the subdiffusive behavior, it tends to preserve the linear behavior for higher frequencies. This result can elucidate experimental data in which changes in the PA signal's linear region are observed and variations in the slope in the exponential decay region.

## Conclusion

The fractional heat conduction and thermal diffusion equations for FDPL for GCE-I were proposed by considering two fractional-order derivatives and two relaxation times from Jeffrey's. We have established the analytical solution, for the temperature profile for a PA problem, by considering a periodic photo-thermal excitation for a homogeneous transparent and opaque sample surrounded by air. The PA signal, *i.e.*, the pressure variation due to the transmission's heat diffusion, is also presented. The GCE-I model is a special case for fractional-order $\beta = 1$ and relaxation time $\tau_T \to 0$. For $\alpha = \beta$ and $\tau_q - \tau_T$, the special case was shown to have the most extreme subdiffusive behavior. We show that the small fractional-order variations in FDPL-GCE-I can modify the subdiffusive to superdiffusive, and vice-versa, depending on $\beta$ and $\tau_T$ values. Thus, this model can influence the PA signal's temperature profile and amplitude and phase delay, even for

Somer, A., *et al.*: Fractional Dual-Phase-Lag Heat Conduction with Periodic ...

2546                                                THERMAL SCIENCE: Year 2023, Vol. 27, No. 3B, pp. 2537-2547

a lower second phase-lag $\tau_T$. These results from the FDPL-GCE-I model are promising to explain experimental results obtained for the open photoacoustic cell technique.

## Acknowledgment

## References

[1]   Pekalski, A., Diffusion Processes: Experiment, Theory, Simulations, Diffusion Processes, in: *Experiment, Theory, Simulations*, Springer, Berlin, Germany, 1994
[2]   Vlahos, L., *et al.*, *Normal and Anomalous Diffusion*: A Tutorial, Patras Univ. Press, On-line first, htpps://doi.org/10.48550/arXiv:0805.0419, 2008
[3]   Liang, L., *et al.*, Magin, A Survey of Models of Ultraslow Diffusion in Heterogeneous Materials, *Appl. Mech. Rev.*, *71* (2019) 040802
[4]   Pekalski, A., Sznajd-Weron, K., *Anomalous Diffusion: From Basics to Applications*, Springer, Berlin, Germany, 1999
[5]   Klafter, J., *et al.*, Stochastic Pathway to Anomalous Diffusion, *Phys. Rev. A*, *35* (1987), 3081
[6]   Block, A., *et al.*, Tracking Ultrafast Hot-Electron Diffusion in Space and Time by Ultrafast Thermomodulation Microscopy, *Science Advances*, *5* (2019), eaav8965
[7]   Mozafarifard, M., Toghraie, D., Time-Fractional Subdiffusion Model for Thin Metal Films under Femtosecond Laser Pulses Based on Caputo Fractional Derivative to Examine Anomalous Diffusion Process, *Int. J. Heat. Mass. Tran.*, *153* (2020), 119592
[8]   Cattaneo, C., Sulla conduzione del calore (in Italian), *Atti Sem. Mat. Fis. Univ. Modena*, *3* (1948), pp. 83-101
[9]   Zhang, W., *et al.*, Time-Fractional Heat Equations and Negative Absolute Temperatures, *Comput. Math. Appl. 67* (2014), 1, pp. 164-171
[10]  Koh, Y. R., *et al.*, Quasi-Ballistic Thermal Transport in Al0.1Ga0.9n Thin Film Semiconductors, *Appl. Phys. Lett.*, *109* (2016), 243107
[11]  Compte, A., Metzler, R., The Generalized Cattaneo Equation for the Description of Anomalous Transport Processes, *Journal Phys. A: Math. and Gen.*, *30* (1997), 21, pp. 7277-7289
[12]  Galovic, S., *et al.*, Theory of Photoacoustic Effect in Media with Thermal Memory, *Journal Appl. Phys. 116* (2014), 024901
[13]  Šoškic, Z., *et al.*, An Extension the Methodology for Characterization of Thermalproperties of Thin Solid Samples by Photoacoustic Techniques, *Int. J. Therm. Sci.*, *109* (2016), Nov., pp. 217-230
[14]  Djordjevic, K., *et al.*, Photo-Thermal Response of Polymeric Materials Including Complex Heat Capacity, *Int. J. Thermophys.*, *43* (2022), 68
[15]  Somer, A., *et al.*, Theoretical Predictions for Photoacoustic Signal: Fractionary Thermal Diffusion with Modulated Light Absorption Source, *Eur. Phys. J. Plus.*, *134* (2019), 18
[16]  Somer, A., *et al.*, Fractional GCES Behaviors Merged: Prediction the Photoacoustic Signal Obtained with Subdiffusive and Superdiffusive Operators, *Journal Appl. Phys.*, *128* (2020), 075107
[17]  Markushev, D., *et al.*, Enhancement of the Thermoelastic Component of the Photoacoustic Signal of Silicon Membranes Coated with a Thin TiO$_2$ Film, *Journal Appl. Phys.*, *131* (2022), 085105
[18]  Popovic, M., Optically Induced Temperature Variations in a Two-Layer Volume Absorber Including Thermal Memory Effects, *Journal Appl. Phys.*, *129* (2021), 015104
[19]  Rosencwaig, A., Gersho, A., Theory of the Photoacoustic Effect with Solids, *Journal Appl. Phys.*, *47* (1976), 1, pp. 64-69
[20]  Perondi, L. F., Miranda, L. C. M., Minimal-Volume Photoacoustic Cell Measurement of Thermal Diffusivity: Effect of the Thermoelastic Sample Bending, *Journal Appl. Phys.*, *62* (1987), 7, pp. 2955-2959
[21]  Somer, A., *et al.*, The Thermoelastic Bending and Thermal Diffusion Processes Influence on Photoacoustic Signal Generation Using Open Photoacoustic Cell Technique, *Journal Appl. Phys.*, *114* (2013), 063503
[22]  Todorovic, D., *et al.*, Photoacoustic Elastic Bending in Thin Film – Substrate System, *Journal Appl. Phys. 114* (2013), 213510
[23]  Nesic, M., P*et al.*, Photo-Thermal Thermoelastic Bending for Media with Thermal Memory, *Int. J. Thermophys.*, *33* (2012), July, pp. 2203-2209
[24]  Awad, E., *et al.*, From Continuous-Time Random Walks to the Fractional Jeffreys Equation: Solution and Properties, *Int. J. Heat. Mass. Tran.*, *181* (2021), 121839

Somer, A., *et al.*: Fractional Dual-Phase-Lag Heat Conduction with Periodic ...
THERMAL SCIENCE: Year 2023, Vol. 27, No. 3B, pp. 2537-2547

2547

[25] Awad, E., Metzler, R., Crossover Dynamics from Superdiffusion Subdiffusion: Models and Solutions, *Fract. Calc. Appl. Anal.*, *23* (2020), Feb., pp. 55-102

[26] Xu, H.-Y., Jiang, X.-Y., Time Fractional Dual-Phase-Lag Heat Conduction Equation, *Chinese Phys. B*, *24* (2015), 034401

[27] Somer, A., *et al.*, Simultaneous Fit of the Photoacoustic Signal Amplitude and Phase for Aisi 316 with Fractional Analysis, On-line first, at SSRN, https://ssrn.com/abstract=4087309 or https://dx.org/10.2139/ssrn.4087309, 2022

[28] Tzou, D., A Unified Field Approach for Heat Conduction from Macro- to Micro-Scales, *Previews of Heat and Mass Transfer*, *2*1 (1995), 196

[29] Singh, S., *et al.*, Three-Phase-Lag Bioheat Transfer Model of Cardiac Ablation, *Fluids*, *7* (2022), 180

[30] Hobiny, A., *et al.*, Analytical Estimation of Temperature in Living Tissues Using the TPL Bioheat Model with Experimental Verification, Mathematics, *8* (2020), 1188

[31] R. Kumar, R., *et al.*, Characterization of Thermal Damage of Skin Tissue Subjected to Moving Heat Source in the Purview of Dual Phase Lag Theory with Memory-Dependent Derivative, *Wave Random Complex*, On-line first, https://doi.org/10.1080/17455030.2021.1979273, 2021

[32] Shomali, Z., *et al.*, Lagging Heat Models in Thermodynamics and Bioheat Transfer: A Critical Review, *Continuum Mech. Therm*., *34* (2022), Apr., pp. 637-679

[33] Lenzi, E. K., *et al.*, Non-Linear Fractional Diffusion Equation: Exact Results, *Journal Math. Phys*., *46* (2005), 083506

[34] Evangelista, L. R., Lenzi, E. K., *Fractional Diffusion Equations and Anomalous Diffusion*, Cambridge University Press, Cambridge, Mass., USA, 2018

[35] Evangelista, L. R., Lenzi, E. K., *An Introduction Anomalous Diffusion and Relaxation*, Springer Nature, Berlin, Germany, 2023

[36] Rousset, G., *et al.*, Influence of Thermoelastic Bending on Photoacoustic Experiments Related to Measurements of Thermal Diffusivity of Metals, *Journal Appl. Phys*., *54* (1983), 5, pp. 2383-2391

[37] Jou, D., *et al.*, *Extended Irreversible Thermodynamics*, Springer, Berlin, Germany, 1996

[38] Somer, A., *et al.*, Anomalous Thermal Diffusion in Two-Layer System: The Temperature Profile and Photoacoustic Signal for Rear Light Incidence, *Int. Jou., of Thermal Science, 179* (2022), Sept., 107561

[39] Galovic, S., Kostoski, D., Photo-Thermal Wave Propagation in Media with Thermal Memory, *Journal Appl. Phys*., *93* (2003), 5, pp. 3063-3070

[40] Popovic, M. N, *et al.*, Photoacoustic Response of a Transmission Photoacoustic Configuration for Two-Layer Samples with Thermal Memory, *Opt. Quant. Electron*., *50* (2018), 330